A Comparative Study of Efficient Offline Single-Stage AC-DC LED Lighting Drivers Across Various Output Ranges

Kunhee Cho
School of Electronic and Electrical Engineering, Kyungpook National University
E-mail : kunhee@knu.ac.kr

***Abstract*—A comparative study is presented on the efficiency of an offline single-stage AC-DC LED driver for various LED strings. To ensure a fair comparison among different types of power converters, averaged switch models of non-isolated LED drivers, based on peak current control, are employed for buck, buck-boost, and boost converters. The averaged switch model allows for easy determination of performance metrics, such as power factor (PF), total harmonic distortion (THD), and output power (POUT). Additionally, it provides a fair means of comparing performance by altering the number of LED strings used with different types of power converters. In this paper, the power boundary of LED strings for each type of power converter is clearly defined, given a constant AC input voltage.**

Keywords— Averaged switch model, AC-DC converter, LED driver, peak current control

I. INTRODUCTION

High-brightness and high-efficiency light-emitting diode (LED) technology is increasingly popular due to its extended lifetime and superior efficiency [1-12]. Furthermore, LEDs are viewed as environmentally friendly devices because they do not contain mercury and emit very low levels of carbon dioxide.

LED drivers for general lighting applications regulate the output power of LEDs derived from the AC outlet. A crucial metric in this power conversion is the power factor (PF), which indicates how efficiently electrical power is transferred from the AC line voltage to the load. Another significant aspect is the total harmonic distortion (THD) of the input AC current. High THD can interfere with other electronic equipment, potentially shortening their lifetimes. To enhance the PF and THD in LED driver applications, an inductor-based switching-type DC-DC converter followed by the power factor correction (PFC) circuit can be utilized. The PFC circuit can be implemented by either through a controller-based active approach or a valley-fill passive method. However, given the elevated manufacturing costs associated with extra PFC circuits, AC-DC converter types of LED drivers have emerged. Unlike DC-DC converters, AC-DC converters can achieve PFC without necessitating an additional PFC circuit, by utilizing a time-varying signal as a control loop reference.

LEDs have been used in both indoor and outdoor lighting applications with varying output power requirements. For optimal performance, the type of power converter should be selected based on the number of LEDs corresponding to the AC line voltage range. Typically, indoor applications demand fewer LEDs than outdoor ones due to lower output power needs. For indoor settings, AC-DC converters often employ step-down conversions, like buck converters [1-4], or step-up/down conversions, such as flyback [5] or buck-boost converters [2], given the relatively few LEDs in use. For higher output power in outdoor settings, which necessitate a larger LED count, both step-up/down and step-up conversions, like boost converters, are suitable. Step-down conversion isn't advisable for extensive LED arrays, especially if the LED's forward voltage exceeds the fluctuating AC input voltage. Although various converter types have been implemented in LED lighting applications [1-5], the appropriate boundaries for each converter type concerning different output power ranges remain undefined.

In this paper, an efficient solution for non-isolated LED drivers across various output power ranges is analyzed, focusing on the buck, buck-boost, and boost converter operations. A guide map for efficient driver solutions is introduced based on LED string counts. Additionally, the averaged switch models for each converter are described, based on peak-current control, to ensure a fair performance comparison under consistent conditions.

This paper is organized as follows. Section II introduces a averaged behavior model of buck, buck-boost, and boost type LED driver. Section III provides the simulated results, and Section IV describes a comparison among various types of LED drivers. Conclusions are provided in Section V.

a. Corresponding author; kunhee@knu.ac.kr

Manuscript Received Sep. 21, 2023, Revised Nov. 21, 2023, Accepted Nov. 28, 2023

This is an Open Access article distributed under the terms of the Creative Commons Attribution Non-Commercial License (http://creativecommons.org/licenses/by-nc/4.0) which permits unrestricted non-commercial use, distribution, and reproduction in any medium, provided the original work is properly cited.

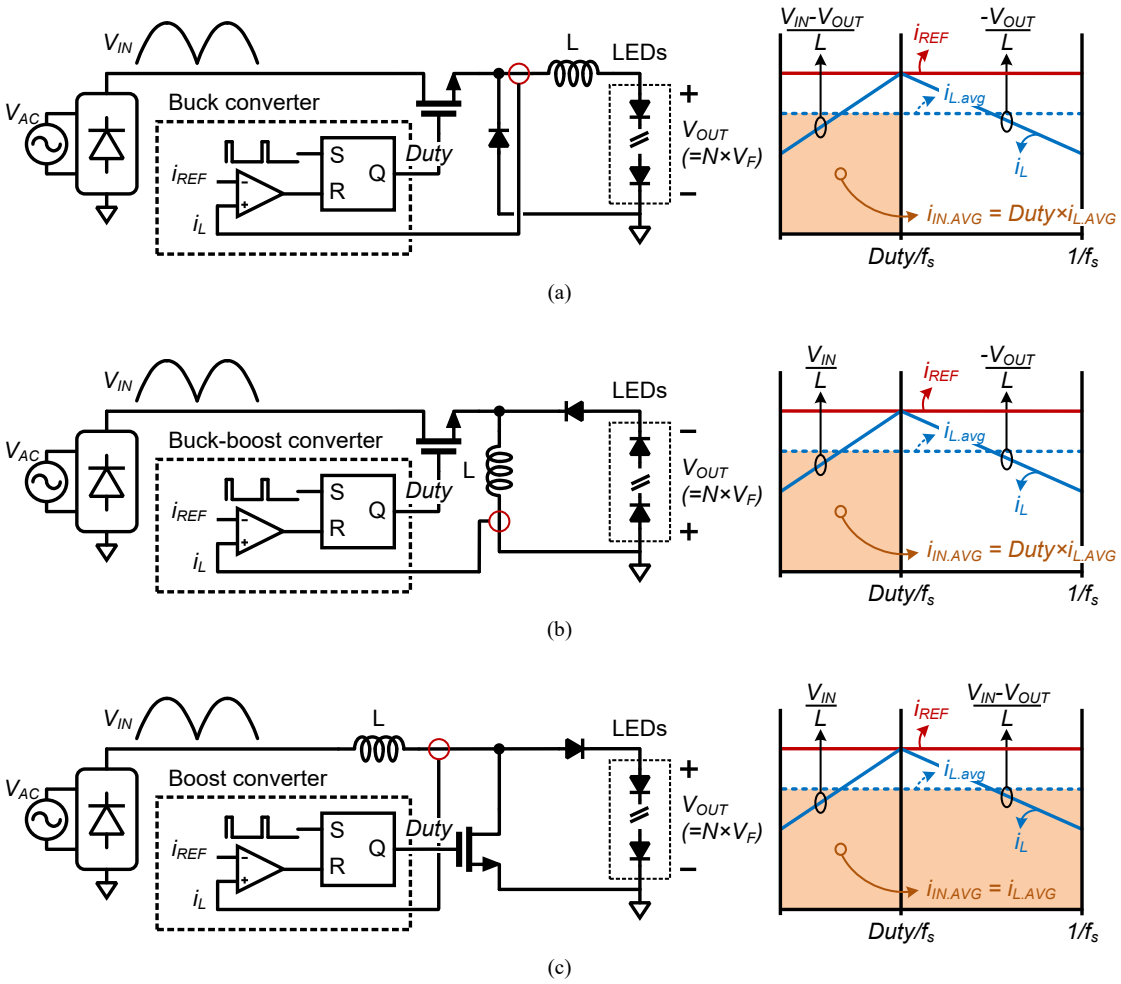

Fig. 1. AC-DC LED driver based on peak current control (a) Buck converter. (b) Buck-boost converter. (c) Boost converter.

II. Averaged Behavior Model of LED Driver

A single-stage, non-isolated LED driver can be implemented using various types of power converters such as buck, buck-boost, and boost converters, as shown in Fig. 1. The converter operates based on a peak current-controlled pulse-width-modulation (PWM) method, which controls the inductor current (i_L) using a current reference (i_{REF}). The sensed inductor current is compared at its peak level to the current reference, which in turn controls the duty cycle (D). Since the given current reference is a time-varying signal, the inductor current follows its form, albeit with some ripple.

To enable a fair comparison under different load conditions, the averaged switch model can be employed for analyzing various LED drivers. Assuming that the buck converter operates in continuous conduction mode (CCM) using a properly sized inductor at a given switching frequency, the averaged switch model for the buck converter can be expressed as follows [13, 14]:

$$L\frac{di_{L.avg}}{dt} = D \cdot V_{IN} - V_{OUT} \quad (1)$$

$$C\frac{dV_{OUT}}{dt} = i_{L.avg} - i_{OUT}$$

where D is the duty-cycle, i_{OUT} is the output current flowing into LEDs, C is the output capacitor between the diode string and $i_{L.avg}$ is the average of the inductor current.

To model the peak current-controlled PWM method within the averaged switch model, the duty cycle for each switching cycle must be calculated to account for the time-varying current reference. Fig. 1(a) (right) depicts the waveform of both the current reference and the inductor current within a single switching period. Even though these are time-varying signals, they can be considered as DC for each switching cycle, given that the switching frequency (f_s) which is usually at a few tens or hundreds of kHz is much higher than the rectified AC line frequency (e.g. 100−120 Hz).

To calculate the duty cycle, the switching inductor current is needed, as the duty cycle is set at the point where the inductor current meets the current reference. Using the averaged switching model, the initial point of the inductor current can be expressed as:

TABLE I
AVERAGED POWER CONVERTERS MODEL BASED ON PEAK CURRENT CONTROL

Type	i_{IN}	i_{OUT}	Avg. switch model	Duty-cycle (D)
Buck converter	Di_L	i_L	$L\frac{di_L}{dt} = DV_{IN} - V_{OUT}$ $C\frac{dV_{OUT}}{dt} = i_L - i_{OUT}$	$\frac{2(i_{REF} - i_L)Lf_S}{V_{IN} - V_{OUT}}$
Buck-boost converter	Di_L	$D'i_L$	$L\frac{di_L}{dt} = DV_{IN} - D'V_{OUT}$ $C\frac{dV_{OUT}}{dt} = D'i_L - i_{OUT}$	$\frac{2(i_{REF} - i_L)Lf_S}{V_{IN}}$
Boost converter	i_L	$D'i_L$	$L\frac{di_L}{dt} = V_{IN} - D'V_{OUT}$ $C\frac{dV_{OUT}}{dt} = D'i_L - i_{OUT}$	$\frac{2(i_{REF} - i_L)Lf_S}{V_{IN}}$

D' = 1-D, C is the output capacitor across the LED string.

$$i_L(0) = i_{REF} - 2\left(i_{REF} - i_{L.avg}\right) = 2i_{L.avg} - i_{REF} \quad (2)$$

Since the rising slope of inductor current at buck converter is ($V_{IN} - V_{OUT}$)/L, the inductor current at variable duty-cycle can be represented as below,

$$i_L(D) = i_L(0) + \frac{(V_{IN} - V_{OUT})}{L} \cdot \frac{D}{f_S} \quad (3)$$

By setting the point when $i_L(D) = i_{REF}$, the duty-cycle of peak current control can be expressed as below,

$$D = \frac{2 \cdot (i_{REF} - i_L) \cdot L \cdot f_S}{V_{IN} - V_{OUT}} \quad (4)$$

Since the input current only flows when the switch is on-state, it shows a discontinuous form. The output LED current (i_{OUT}) is equal to the inductor current in the buck converter. Therefore, the input current and the output current can be expressed as below,

$$\begin{aligned} i_{IN} &= D \cdot i_L \\ i_{OUT} &= i_L \end{aligned} \quad (5)$$

where, i_{IN} is the input current from rectified input voltage and i_{OUT} is the LED current.

III. SIMULATION RESULTS

Fig. 2 illustrates the simulated waveforms of each power converter based on the averaged switch model. These simulations were conducted using the Cadence Spectre tool. An input voltage of 110 VAC was applied, and the output power was adjusted by using a varying number of LEDs. The inductor current in all cases emulates a sine-wave form due to the peak current control with a sine-wave current reference (i_{REF}). The maximum duty-cycle is capped at 0.8 for practical implementation considerations.

Fig. 2 (a) presents the simulated waveform of the buck converter, which has a peak output voltage of 16 V. The output current mirrors the sine-wave form, identical to the inductor current. In this scenario, the PF and THD are 0.941 and 29.5% respectively. Due to the step-down power conversion topology, the output voltage fails to sustain the forward voltage of the diode at low input voltages. This

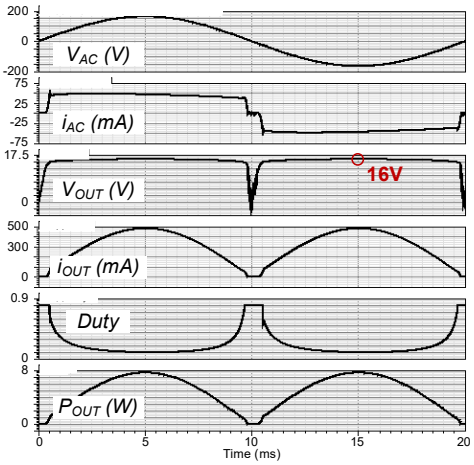

(a)

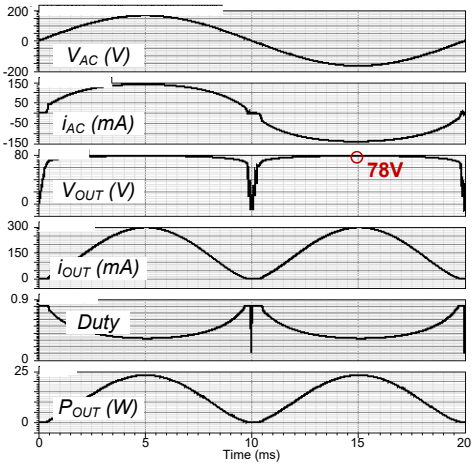

(b)

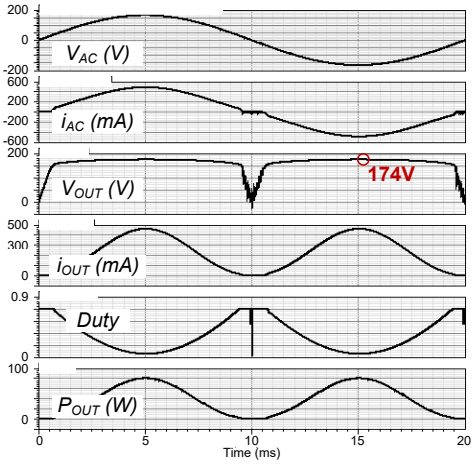

(c)

Fig. 2. Simulated waveform with sine-wave reference control. (a) Buck converter. (b) Buck-boost converter. (c) Boost converter.

segment is referred to as the "dead zone", which expands as the number of LEDs increase.

Fig. 2 (b) shows the simulated waveform of the buck-boost converter, which achieves a peak output voltage of 78 V.

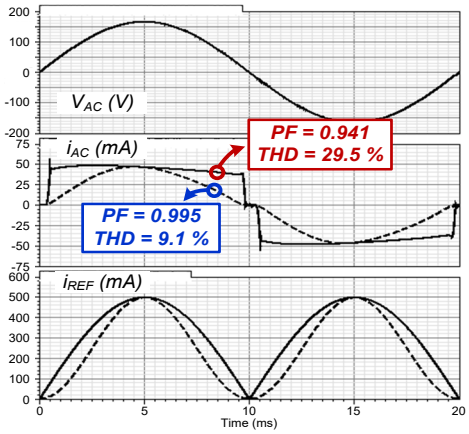

(a)

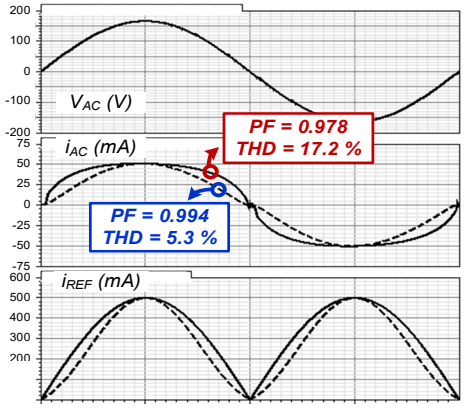

(b)

Fig. 3. Simulated waveform with different reference control. Solid line shows the sine-wave reference control and dashed line shows the reference control proposed in [2]. (a) Buck converter. (b) Buck-boost converter.

Contrary to the buck converter, the buck-boost converter can both step up and step down the output voltage in relation to the input. As a result, it can drive a larger number of LEDs compared to the buck converter. The conversion ratio for the buck-boost converter is defined as D/(1-D), and it is limited to 4 given that the maximum duty-cycle is set to 0.8. In this instance, the PF and THD values are 0.992 and 11.1% respectively.

Fig. 2 (c) shows the simulated waveform of the boost converter, where the peak output voltage reaches 174 V. Here, the PF and THD are 0.997 and 8.1% respectively. The forward voltage of the LEDs must exceed the input's peak voltage since the boost converter only facilitates up-conversion.

One advantage of the averaged switch model is that it allows for the straightforward extraction of output results under various parameter conditions and for different forms of the current reference (i_{REF}). The PF and THD can be improved by applying the current reference of the $\sin^2$ function for the buck converter, and the reference of $\alpha \cdot \sin + (1-\alpha) \cdot \sin^2$ function where α is a $V_{OUT.PEAK}/(V_{OUT.PEAK}+V_{AC.PEAK})$ for the buck-boost converter [2]. Fig. 3 shows the simulated waveform with the current reference proposed in [2] (dashed line) compared to the sine-wave current reference form (solid line). The PF and THD are enhanced significantly for both buck and buck-boost converters by applying the proposed reference in [2], and the shape of the input current is closer to the sine-waveform.

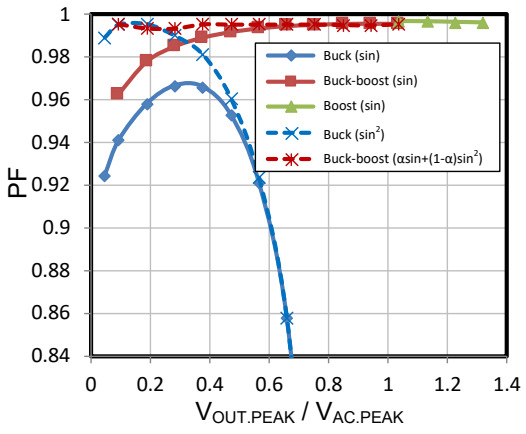

(a)

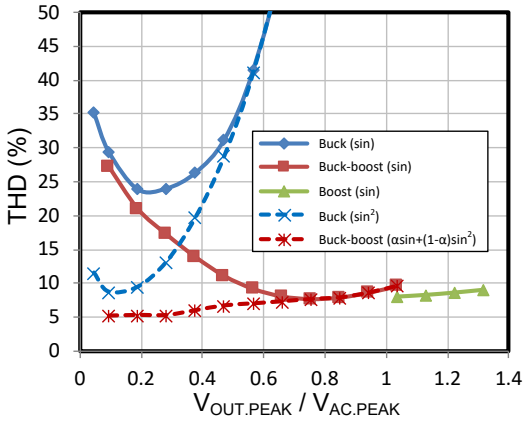

(b)

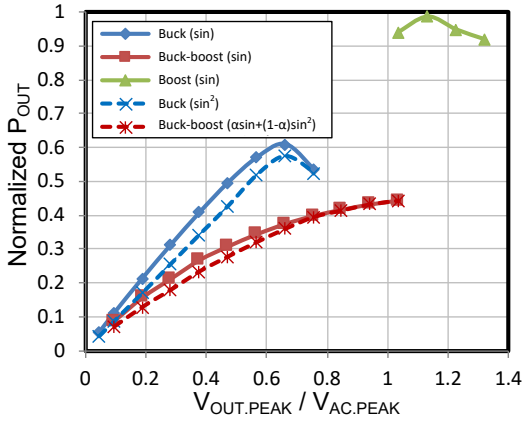

(c)

Fig. 4. Performance results. (a) PF. (b) THD. (c) P_{OUT}.

IV. Performance Comparison

Fig. 4 compares the performance of each power converter while varying the number of LEDs. Although the buck converter exhibits a higher P_{OUT} than the buck-boost

TABLE II
PERFORMANCE SUMMARY

	$\frac{V_{OUT.PEAK}}{V_{AC.PEAK}}$	Min. PF	Max. THD	Norm. $P_{OUT.MAX}$
Buck converter†	< 0.28	0.99	13.1 %	0.26
Buck-boost converter†	< 1	0.995	9.5 %	0.45
Boost converter	> 1	0.996	8.9 %	1.0

Performance comparison has been made that can obtain PF > 0.99.

†Current reference of $\sin^2$ and $\alpha \cdot \sin + (1-\alpha) \cdot \sin^2$ function is used here for the buck and buck-boost converter, respectively [2].

converter at the same V_{OUT} level due to its continuous output current flow, its PF and THD deteriorate rapidly as the output voltage rises. This is attributed to the expanding range of the dead zone. To achieve a PF above 0.99, the buck converter is suitable for a $V_{OUT.PEAK}/V_{AC.PEAK}$ ratio of under 0.28. For ratios above 0.28, the buck-boost converter should be used. Additionally, the buck-boost converter operates over a broader range of V_{OUT} and offers better performance than the buck converter. The boost converter, on the other hand, can attain the highest P_{OUT} but is limited to operating above the input voltage (V_{AC}) range. For the boost converter, a higher V_{OUT} doesn't substantially increase the P_{OUT}, owing to the duty-cycle limitation. When comparing the buck-boost and boost converters at an equivalent V_{OUT} level, the boost converter demonstrates approximately double the P_{OUT} of the buck-boost converter. As a result, the inductor current level for the boost converter can be reduced by half to match the output power of the buck-boost converter. Table II provides a summary of the performance of each power converter, detailing their optimal operating ranges to maintain a PF above 0.99.

V. CONCLUSION

This study compares efficient single-stage AC-DC LED drivers using the averaged switch models of power converters based on peak current control. From a fair comparison of results, it is evident that the buck converter is optimal for LED string peaks less than 0.28 of $V_{AC.PEAK}$ to maintain a PF above 0.99. The buck-boost converter can be employed up to the point where the LED string peak reaches $V_{AC.PEAK}$. For LED string peaks surpassing $V_{AC.PEAK}$, the boost converter is the preferred choice, offering the advantage of significantly reduced inductor current compared to the buck-boost converter.

ACKNOWLEDGEMENT

This work was supported by the NRF, grant funded by the Korea government (MSIT) (No. 2021R1C1C1004596). The EDA tool was supported by the IC Design Education Center (IDEC), Korea.

REFERENCES

[1] J. T. Hwang, K. Cho, D. Kim, M. Jung, G. Cho, and S. Yang, "A simple LED lamp driver IC with intelligent power-factor correction," in *IEEE ISSCC Dig.Tech. Papers*, Feb. 2011, pp. 236–238.

[2] K. Cho and R. Gharpurey, "An efficient buck/buck-boost reconfigurable LED driver employing SIN^2 Reference," *IEEE J. Solid-State Circuits*, vol. 52, no. 10, pp. 2758–2768, Oct. 2017.

[3] C. Shin *et al.*, "Sine-reference band (SRB)-controlled average current technique for phase-cut dimmable AC–DC buck LED lighting driver without electrolytic capacitor," *IEEE Trans. Power Electron.*, vol. 33, no. 8, pp. 6994–7009, Aug. 2018.

[4] S. Bandyopadhyay, B. Neidorff, D. Freeman, and A. P. Chandrakasan, "90.6% efficient 11MHz 22W LED driver using GaN FETs and burst-mode controller with 0.96 power factor," in *IEEE ISSCC Dig. Tech. Papers*, Feb. 2013, pp. 368–369.

[5] S. Jung and G. H. Cho, "Transformer coupled recycle snubber for high efficiency offline isolated LED driver with on-chip primary-side power regulation," *IEEE Trans. Ind. Electron.*, vol. 61, no. 12, pp. 6710–6719, Dec. 2014.

[6] W. Hong, M. Lee, "A current-mode DC-DC boost converter for automotive LED headlamp driver," *IDEC Journal of Integrated Circuits and Systems*, vol. 6, no.3, Jul. 2020, pp. 1–6.

[7] J. T. Hwang, M. S. Jung, D. H. Kim, J. H. Lee, M. H. Jung, and J. H. Shin, "Off-the-line primary side regulation LED lamp driver with single-stage PFC and TRIAC dimming using LED forward voltage and duty variation tracking control," *IEEE J. Solid-State Circuits*, vol. 47, no. 12, pp. 3081–3094, Dec. 2012.

[8] L. Li, Y. Gao, H. Jiang, P. K. T. Mok, and K. M. Lau, "An auto-zero voltage-switching quasi-resonant LED driver with GaN FETs and fully integrated LED shunt protectors," *IEEE J. Solid-State Circuits*, vol. 53, no. 3, pp. 913–923, Mar. 2018.

[9] L. Li, Y. Gao, P. K. T. Mok, I.-S.-M. Sun, and N. Park, "A 16–28-W 92.8%-efficiency monolithic quasi-resonant LED driver with constantduty-ratio frequency regulator," *IEEE Trans. Circuits Syst. II, Exp.Briefs*, vol. 62, no. 12, pp. 1199–1203, Dec. 2015.

[10] L. Cheng et al., "On-chip compensated wide output range boost converter with fixed-frequency adaptive off-time control for LED driver applications," *IEEE Trans. Power Electron.*, vol. 30, no. 4, pp. 2096–2107, Apr. 2015.

[11] S. Jung and G.-H. Cho, "Transformer coupled recycle snubber for highefficiency offline isolated LED driver with on-chip primary-side power regulation," *IEEE Trans. Ind. Electron.*, vol. 61, no. 12, pp. 6710–6719, Dec. 2014.

[12] C.-Y. Hsieh and K.-H. Chen, "Boost DC-DC converter with fast reference tracking (FRT) and charge-recycling (CR) techniques for highefficiency and low-cost LED driver," *IEEE J. Solid-State Circuits*, vol. 44, no. 9, pp. 2568-2580, Sep. 2009.

[13] R. D. Middlebrook and S. Cuk, "A general unified approach to modeling switching converter power stages," in *Proc. IEEE Power Electron. Specialist Conf.*, 1976, pp. 18–34.

[14] J. Mahdavi, A. Emaadi, M. D. Bellar and M. Ehsani, "Analysis of power electronic converters using the generalized state-space averaging approach," *IEEE Trans. Circuits Syst. I, Fundam. Theory Appl.*, vol. 44, no. 8, pp. 767–770, Aug. 1997.

Kunhee Cho received the B.S. and M.S. degrees in electrical and electronic engineering from Yonsei University, Seoul, South Korea, in 2007 and 2009, respectively, and the Ph.D. degree in electrical and computer engineering from the University of Texas at Austin, Austin, TX, USA, in 2016.

From 2009 to 2012, he was with the Fairchild Semiconductor,

Bucheon, South Korea, where he designed power management integrated circuits (ICs). In 2015 and 2016, he was a Graduate Research Intern with the Texas Instruments Incorporated, Dallas, TX, USA, in the low-power RF team. From 2017 to 2019, he was with Qualcomm Technologies Incorporated, Santa Clara, CA, USA, where he designed power management ICs for battery charger systems. He is currently an Assistant Professor at the School of Electronics Engineering, Kyungpook National University, Daegu, South Korea. His research interests include power management ICs, gate drivers, class-D amplifiers, and RF power amplifiers.

Dr. Cho was a recipient of the Texas Instruments Outstanding Student Design Award in 2013.